ARTICLES

Damped stochastic system driven by colored noise: Analytical solution by a path integral approach

Chitralekha Mahanta*
Department of Electrical Engineering, Indian Institute of Technology, Delhi Hauz Khas, New Delhi 110 016, India

T. G. Venkatesh†
Department of Electrical Engineering, Indian Institute of Technology, Madras Chennai-600 036, India
(Received 8 April 1999)

We consider the nonlinear non-Markovian stochastic process associated with the damped nonlinear dynamical system driven by Ornstein-Uhlenbeck noise. An approximate Fokker-Planck-type equation governing the above stochastic process is derived using the path-integral approach. The stationary probability density function (SPDF) of the above process is then computed using the matrix continued fraction method. The SPDF compares favorably with the corresponding digital simulation results obtained by us.

PACS number(s): 05.40.−a

I. INTRODUCTION

Stochastic differential equations (SDE's), also known as Langevin equations in physical literature, play an important role in modeling a variety of stochastic phenomena occurring in physics, chemistry, engineering, biology, and medicine [1–3]. In condensed-matter physics, many problems including superionic conduction [4], soliton dynamics [3], diffusion of atoms at crystal surfaces [5], phase-locked loop devices [2], a driven Ge photoconductor [6], nematic liquid crystals [7], and superfluid helium [8] can be described by SDE's. Dye lasers [9], ring-laser gyroscopes [10], and optical computing devices [11] are some of the examples in optical physics modeled by SDE's. Reaction-rate theory [12] and photochemistry [13] are two of the examples in chemistry described by SDE's. In engineering, one encounters SDE's while modeling Josephson junctions [2], electronic oscillators [14], and nuclear reactors [15]. The human immune system [16], genetic models [17], neuronal modeling [18], the motion of organisms like cells or bacterias [19] and transport phenomena in proteins [20] are some of the biological systems satisfactorily described by SDE's.

We consider the SDE describing the Brownian motion of a particle of unit mass in a one-dimensional potential $U(x)$ described by the Langevin equation

$$\ddot{x} = -\gamma\dot{x} - \frac{dU(x)}{dx} + \xi(t), \tag{1}$$

where x is the position of the Brownian particle, γ is the damping coefficient, and $\xi(t)$ is the noise. In Eq. (1) overdots represent derivatives with respect to time.

When the noise driving a SDE is a δ-correlated white noise, i.e., $\langle \xi(t)\xi(s)\rangle = 2D\,\delta(t-s)$, where D is the noise strength, the solution process $x(t)$ is a Markov process. Markov processes are well described by Fokker-Planck equations (FPEs) [2]. However, noise encountered in reality has a nonzero correlation time, and hence is called colored noise. Colored noise is modeled quite well by the Ornstein-Uhlenbeck (OU) process, which is a Gaussian Markovian process [21]. For this case, the two time correlation function of $\xi(t)$ is given by $\langle \xi(t)\xi(s)\rangle = (D/\tau)\exp(-|t-s|/\tau)$, where D is the noise strength, τ is the noise correlation time, and the angular brackets represent ensemble averaging. When the noise driving the SDE is colored, the nature of the stochastic process becomes non-Markovian. Standard Fokker-Planck techniques are not applicable for non-Markovian processes. The study of nonlinear stochastic systems driven by colored noise has been undertaken by a number of investigators (for a review, please see Ref. [3]). Most of the theoretical approaches proposed so far consider the overdamped limit, and try to describe the non-Markov process using an approximate FPE. Such Fokker-Planck approximations arise as a result of using functional calculus [22], cumulant summation [23], projection operator technique [24], the matrix continued fraction method, (MCF) [2,25], and the path integral [26–29] technique. In particular, the path integral method has proven to be a good technique in the weak noise limit. The path integral method has yielded good results in the study of an overdamped bistable potential driven by OU noise for important statistical quantities like the mean first passage time and the stationary probability density function (SPDF) [30]. For the case of finite damping, the Langevin equation can be written as a three-dimensional Markovian process. An analytical treatment of this equation is extremely difficult because of its following characteristics: (a) nonlinearity, (b) non-Markovicity, and (c) lack of detailed balance. Apart from some analog [31] and digital [32] simulation studies, there has been very little analytical work dealing with the problem of a damped stochastic system driven by colored noise.

*Department of Electronics and Communication Engineering, Indian Institute of Technology, Guwahati 781001, India. Electronic address: chitra@ee.iitd.ernet.in

†Electronic address: tgvenky@ee.iitm.ernet.in

Fronzoni *et al.* [33] used projector-operator technique to obtain an approximate, nonlinear Fokker-Planck-type equation for a colored noise driven damped bistable system. Fronzoni *et al.* computed the SPDF $P(x)$, and compared the theoretical results with their digital and analog simulation results. Recently, the authors of Ref. [34] considered a Langevin equation driven by colored noise with an inertial term, and derived the extremal action analytically using the path integral method. The present paper proposes an approximate theoretical solution to the colored noise driven stochastic system with finite damping. We derive an approximate FPE for the above process using the path integral technique. We also calculate the SPDF of the colored noise driven damped stochastic system.

The paper is organized as follows: In Sec. II, we derive an approximate FPE using the path integral method. We also derive effective diffusion coefficients associated with the FPE using the steepest descent technique. In Sec. III, we use the MCF method and derive a formula for calculating the SPDF. In order to validate our theoretical results, in Sec. IV we do a case study of a damped bistable potential driven by colored noise. In our case study, we first numerically compute the minimal action path (MAP), and then compute the effective diffusion coefficients present in our approximate FPE. Next the SPDF of the x process is calculated and compared with that of corresponding digital simulation results. Section V contains our conclusions.

II. APPROXIMATE FOKKER-PLANCK EQUATION: PATH INTEGRAL METHOD

In this section we derive an approximate FPE governing Eq. (1) using the path integral technique. We start with the exact master equation for Eq. (1) obtained by using the functional derivative technique [22,35,36]. The master equation is [see Eq. (3.1) of Ref. [33]]

$$\frac{\partial P(x,\nu,t)}{\partial t}=\frac{\partial}{\partial t}\langle\delta(x(t)-x)\,\delta(\nu(t)-\nu)\rangle \tag{2}$$

$$\begin{aligned}=&-\nu\frac{\partial}{\partial x}P(x,\nu,t)+U'(x)\frac{\partial}{\partial\nu}P(x,\nu,t)+\gamma\frac{\partial}{\partial\nu}[\nu P(x,\nu,t)]\\&+\frac{\partial^2}{\partial\nu\partial x}\left[\frac{D}{\tau}\int_0^t ds\exp\left[-\frac{(t-s)}{\tau}\right]\left\langle\delta(x(t)-x)\delta(\nu(t)\right.\right.\\&\left.\left.-\nu)\frac{\delta x(t)}{\delta\xi(s)}\right\rangle\right]+\frac{\partial^2}{\partial\nu^2}\left[\frac{D}{\tau}\int_0^t ds\exp\left[-\frac{(t-s)}{\tau}\right]\left\langle\delta(x(t)\right.\right.\\&\left.\left.-x)\delta(\nu(t)-\nu)\frac{\delta\nu(t)}{\delta\xi(s)}\right\rangle\right].\end{aligned} \tag{3}$$

The ensemble average represented by the angular brackets $\langle\,\rangle$ in Eq. (3) can be replaced by the equivalent path integral notation [22]

$$\begin{aligned}\frac{\partial P(x,\nu,t)}{\partial t}=&-\nu\frac{\partial}{\partial x}P(x,\nu,t)+U'(x)\frac{\partial}{\partial\nu}P(x,\nu,t)\\&+\gamma\frac{\partial}{\partial\nu}[\nu P(x,\nu,t)]+\frac{\partial^2}{\partial\nu\partial x}\left[\frac{D}{\tau}\int_0^t ds\right.\\&\times\exp\left[-\frac{(t-s)}{\tau}\right]\int_-^-\int D[\xi(t)]P[\xi(t)]\delta(x(t)\\&\left.-x)\delta(\nu(t)-\nu)\frac{\delta x(t)}{\delta\xi(s)}\right]+\frac{\partial^2}{\partial\nu^2}\left[\frac{D}{\tau}\int_0^t ds\right.\\&\times\exp\left[-\frac{(t-s)}{\tau}\right]\int_-^-\int D[\xi(t)]P[\xi(t)]\\&\left.\times\delta(x(t)-x)\delta(\nu(t)-\nu)\frac{\delta\nu(t)}{\delta\xi(s)}\right].\end{aligned} \tag{4}$$

In Eq. (4), $\int_-^-\int$ represents the path integral over $\xi(t)$, $D[\xi(t)]$ is the measure for path integration, and $P[\xi(t)]$ is the probability of occurrence of $\xi(t)$ realization.

Our next step is to evaluate the response functions $\delta x(t)/\delta\xi(s)$ and $\delta\nu(t)/\delta\xi(s)$ in Eq. (4). We use the results presented by Ramirez-Piscina and Sancho in Ref. [37] for our purpose. These authors considered a multivariable system driven by an OU noise given by stochastic differential equations

$$\dot q_\alpha(t)=\nu_\alpha(\mathbf{q}(t))+g_{\alpha\sigma}(\mathbf{q}(t))\xi_\sigma(t), \tag{5}$$

where

$$\langle\xi_\mu(t)\rangle=0, \tag{6a}$$

and

$$\langle\xi_\mu(t)\xi_\nu(s)\rangle=\frac{D_\mu}{\tau_\mu}\delta_{\mu\nu}\exp(-|t-s|/\tau_\mu). \tag{6b}$$

For Eqs. (5) and (6), the response function matrix $\underline{R}(t,s)$ with elements $R_{\alpha\beta}(t,s)=[\delta q_\alpha(t)/\delta\xi_\beta(s)]$ was derived in Ref. [37] to be

$$\underline{R}(t,s)=T\left[\exp\left[\int_s^t ds(\underline{W}+\underline{H})\right]\right]\underline{g}(s), \tag{7}$$

where T is the time-ordering operator and $\underline{g}$ is a matrix with elements $g_{\mu\nu}(\mathbf{q})$. $\underline{W}$ and $\underline{H}$ are matrices with elements g:

$$W_{\alpha\beta\mu\nu}=\frac{\partial\nu_\alpha}{\partial q_\mu}\delta_{\beta\nu}, \tag{8}$$

$$H_{\alpha\beta\mu\nu}=\frac{\partial g_{\alpha\sigma}}{\partial q_\mu}\delta_{\beta\nu}\xi_\sigma. \tag{9}$$

In order to use the above results of Ref. [37], we first convert Eq. (1) to two-dimensional equations:

$$\dot x=\nu, \tag{10a}$$

$$\dot\nu=-U'(x)-\gamma\nu+\xi(t). \tag{10b}$$

For our system, it can be shown that the response function matrix is

$$\underline{R}=\begin{bmatrix} 0 & \dfrac{\delta x(t)}{\delta \xi(s)} \\ 0 & \dfrac{\delta \nu(t)}{\delta \xi(s)} \end{bmatrix}. \tag{11a}$$

Similarly, $\underline{g}$, $\underline{W}$, and $\underline{H}$ are given by

$$\underline{g}=\begin{bmatrix} 0 & 0 \\ 0 & 1 \end{bmatrix}, \tag{11b}$$

$$\underline{W}=\begin{bmatrix} 0 & 1 \\ -U''(x) & -\gamma \end{bmatrix}, \tag{11c}$$

$$\underline{H}=\begin{bmatrix} 0 & 0 \\ 0 & 0 \end{bmatrix}. \tag{11d}$$

Keeping terms only up to first order in $(t-s)$ in Eq. (7), it can be shown that

$$\underline{R}(t,s)=\begin{bmatrix} 0 & (t-s) \\ 0 & 1-\gamma(t-s) \end{bmatrix}, \tag{12}$$

$$\approx\begin{bmatrix} 0 & \exp\int_s^t ds-1 \\ 0 & \exp\int_s^t -\gamma\, ds \end{bmatrix}. \tag{13}$$

Now, comparing Eqs. (11a) and (13), we have

$$\frac{\delta x(t)}{\delta \xi(s)}=\exp\int_s^t ds-1 \tag{14a}$$

and

$$\frac{\delta \nu(t)}{\delta \xi(s)}=\exp\int_s^t -\gamma\, ds. \tag{14b}$$

Substituting Eqs. (14) into Eq. (4), we obtain

$$\begin{aligned}\frac{\partial P(x,\nu,t)}{\partial t}=&-\nu\frac{\partial}{\partial x}P(x,\nu,t)+U'(x)\frac{\partial}{\partial \nu}P(x,\nu,t)\\ &+\gamma\frac{\partial}{\partial \nu}[\nu P(x,\nu,t)]\\ &+\frac{\partial^2}{\partial \nu\partial x}\int_-^- \int D[\xi(t)]P[\xi(t)]\delta(x(t)\\ &-x)\delta(\nu(t)-\nu)\int_0^t ds\frac{D}{\tau}\exp\left[\int_s^t -\tau^{-1}dr\right]\\ &\times\left[\exp\int_s^t dr\ -1\right]\\ &+\frac{\partial^2}{\partial \nu^2}\int_-^- \int D[\xi(t)]P[\xi(t)]\delta(x(t)-x)\delta(\nu(t)\\ &-\nu)\int_0^t ds\frac{D}{\tau}\exp\left[-\int_s^t(\tau^{-1}+\gamma)dr\right].\end{aligned} \tag{15}$$

In order to do the path integration in Eq. (15), we use the fact that $\int_-^- \int D[\xi(t)]P[\xi(t)]=\int_-^- \int D[x(t)]P[x(t)]$. The path probability $P[\xi(t)]$ for the OU process under consideration over the time interval $(0,t)$ is given by [27]

$$P[\xi(t)]\propto\exp\left[\frac{-1}{4D}\int_0^t du[\xi(u)+\tau\dot{\xi}(u)]^2\right]. \tag{16}$$

When $x(t)$ and $\xi(t)$ are related through Eq. (1), we have

$$P[x(t)]\propto J[x(t)]\exp\left(-\frac{S[x(t)]}{D}\right), \tag{17}$$

when action $S[x(t)]$ is given by

$$\begin{aligned}S[x(t)]=\tfrac{1}{4}\int_0^t dt[\{\ddot{x}+\gamma\dot{x}+U'(x)\}^2+\tau^2\{\dddot{x}+\gamma\ddot{x}\\ +U''(x)\dot{x}\}^2].\end{aligned} \tag{18}$$

$J[x(t)]$ is the Jacobian of transformation from the $\xi(t)$ realization to the $x(t)$ realization over the same time interval $(0,t)$.

In the limit $D\to 0$, $P[x(t)]$ given in Eq. (17) reaches a maximum when action $S[x(t)]$ is minimum. Thus, in the limit $D\to 0$, the major contribution to the path integral arises around the MAP which minimizes the action $S[x(t)]$ in reaching $x(t)=x$ from $x(0)$. The condition for minimizing the action is

$$\frac{\delta S[x(t)]}{\delta x(t)}=0. \tag{19}$$

For $S[x(t)]$ given by Eq. (18), the condition given in Eq. (19) yields the fourth order nonlinear ordinary differential equation in y [34]:

$$\begin{aligned}&U'^2-y^2\gamma^2+2U''y^2+y^2(y'^2+2yy'')\\ &\quad=\tau^2\{-y^2(\gamma^2y'^2+2\gamma^2yy''+2\gamma yU'''-U''^2)\\ &\qquad+2y^2(2yy''U''+y'^2U''+2yy'U'''+y^2U''''')\\ &\qquad+y^2(9y^2y''^2+y'^4+16yy'^2y''+12y^2y'y'''+2y^3y''''')\}.\end{aligned} \tag{20}$$

The MAP is the solution of Eq. (20) with suitable boundary conditions. In Eq. (20), y represents $\dot{x}$ and dashes represent derivatives with respect to x.

Let us now consider the two terms

$$\int_0^t ds\frac{D}{\tau}\exp\left[\int_s^t -\tau^{-1}dr\right]\left[\exp\int_s^t dr-1\right]$$

and

$$\int_0^t ds\frac{D}{\tau}\exp\left[-\int_s^t(\tau^{-1}+\gamma)dr\right]$$

in Eq. (15), and invoke the steepest-descent approximation [26], which is valid in the limit $D\to 0$. According to this approximation, we evaluate the above terms along the MAP and take these terms out of the path integral. On performing the remaining path integral in Eq. (15), they simply yield $P(x,v,t)$. Therefore, we propose the effective diffusion coefficients in the small D limit as

$$\int_0^t ds\,\frac{D}{\tau}\exp\left[\int_s^t -\tau^{-1}dr\right]\left[\exp\int_s^t dr-1\right] \tag{21a}$$

and

$$\int_0^t ds\,\frac{D}{\tau}\exp\left[-\int_s^t(\tau^{-1}+\gamma)dr\right], \tag{21b}$$

where the above two terms are evaluated along the MAP. We now go ahead and simplify expression (21) as follows.

Let $z(s)$ and $w(r)$ represent the values of x along the MAP at times s and r respectively. Let $y(z)$ and $y(w)$ represent the velocity variable y along the MAP, defined by Eq. (20) at the spatial points z and w, respectively. Using the relations $y(z)=dz(s)/ds$ and $y(w)=dw(r)/dr$ in expressions (21), we change the time variables s and r into space variables z and w, respectively. Now the diffusion coefficients given by expressions (21a) and (21b) can be written as

$$D_1(x)=\int_{x(0)}^{x(t)}\frac{dz}{y(z)}\,\frac{D}{\tau}\exp\left[\int_z^x -\tau^{-1}\frac{dw}{y(w)}\right]\left[\exp\int_z^x\frac{dw}{y(w)}-1\right] \tag{22a}$$

and

$$D_2(x)=\int_{x(0)}^{x(t)}\frac{dz}{y(z)}\,\frac{D}{\tau}\exp\left[-\int_z^x(\tau^{-1}+\gamma)\,\frac{dw}{y(w)}\right], \tag{22b}$$

respectively.

Substituting these terms $D_1(x)$ and $D_2(x)$ given by Eqs. (22a) and (22b) into Eq. (15), we obtain

$$\begin{aligned}\frac{\partial P(x,\nu,t)}{\partial t}=&-\nu\frac{\partial}{\partial x}P(x,\nu,t)+U'(x)\frac{\partial}{\partial\nu}P(x,\nu,t)\\&+\gamma\frac{\partial}{\partial\nu}\nu P(x,\nu,t)+\frac{\partial^2}{\partial\nu\partial x}D_1(x)P(x,\nu,t)\\&+\frac{\partial^2}{\partial\nu^2}D_2(x)P(x,\nu,t).\end{aligned} \tag{23}$$

This is our effective Fokker-Planck equation (EFPE) with effective diffusion coefficients $D_1(x)$ and $D_2(x)$ given by Eqs. (22a) and (22b), where $y(z)$ and $y(w)$ represent the velocity variable y along the MAP, defined by Eq. (20) at the points z and w, respectively.

III. STATIONARY PROBABILITY DENSITY FUNCTION

In this section we calculate the SPDF for damped stochastic system driven by OU noise [Eq. (10)]. We start with our approximate Fokker-Planck-type equation given by Eq. (23), and rewrite it as follows:

$$\begin{aligned}\frac{\partial P(x,\nu,t)}{\partial t}=&-\nu\frac{\partial}{\partial x}P(x,\nu,t)+\frac{\partial}{\partial\nu}\Big[\gamma\nu+\frac{\partial}{\partial x}\{U(x)\\&+D_1(x)\}\Big]P(x,\nu,t)+D_2(x)\frac{\partial^2}{\partial\nu^2}P(x,\nu,t).\end{aligned} \tag{24}$$

Now let us consider a damped stochastic system driven by white Gaussian noise. Such a system is described by the two-dimensional equations

$$\dot{x}=\nu, \tag{25a}$$

$$\dot{\nu}=-U'(x)-\gamma\nu+\xi(t), \tag{25b}$$

where

$$\langle\xi(t)\rangle=0 \tag{26a}$$

and

$$\langle\xi(t)\xi(s)\rangle=2D\delta(t-s). \tag{26b}$$

The FPE describing the system given by Eq. (25) reads [2]

$$\begin{aligned}\frac{\partial P(x,\nu,t)}{\partial t}=&-\nu\frac{\partial}{\partial x}P(x,\nu,t)+\frac{\partial}{\partial\nu}\Big[\gamma\nu+\frac{\partial}{\partial x}U(x)\Big]P(x,\nu,t)\\&+\gamma\nu_{\rm th}^2\frac{\partial^2}{\partial\nu^2}P(x,\nu,t),\end{aligned} \tag{27}$$

where $\nu_{\rm th}=\sqrt{D/\gamma}=\sqrt{kT}$ is the thermal velocity. We compare the expressions given by Eqs. (24) and (27), and find that they are analogous. The term $\{U(x)+D_1(x)\}$ in Eq. (24) is analogous to the term $U(x)$ in Eq. (27). The term $D_2(x)$ in Eq. (24) is analogous to the term $\gamma\nu_{\rm th}^2$ in Eq. (27).

Risken [2] applied the MCF method to the FPE [Eq. (27)] to derive the SPDF analytically as follows. The SPDF in position is related to the first expansion coefficient of the Brinkman's hierarchy through

$$P(x)=\exp[-\varepsilon U(x)/\nu_{\rm th}^2]C_0(x). \tag{28}$$

Brinkman's hierarchy for the coefficients $C_n(x,t)$ ($C_n=0$ for $n<0$) is given by the set of equations

$$\frac{\partial C_n}{\partial t}=-\sqrt{n}\hat{D}C_{n-1}-n\gamma C_n-\sqrt{n+1}DC_{n+1}, \tag{29}$$

where

$$D=\nu_{\rm th}\frac{\partial}{\partial x}-\varepsilon\,\frac{dU(x)}{dx}\Big/\,\nu_{\rm th} \tag{30}$$

and

$$\hat{D}=\nu_{\rm th}\frac{\partial}{\partial x}+(1-\varepsilon)\,\frac{dU(x)}{dx}\Big/\,\nu_{\rm th}. \tag{31}$$

In the stationary state, a general solution of Eq. (29) is easily obtained for the case where the probability current in x direction integrated over the velocities vanishes, i.e., $C_1=0$. This solution is given by

$$\hat{D}C_0=0, \tag{32}$$

i.e.,

$$C_0(x)\sim\exp[-(1-\varepsilon)U(x)/\nu_{\rm th}^2], \tag{33}$$

and $C_n=0$ for $n\geqslant 1$. Substituting Eq. (33) into Eq. (28), Risken obtained

$$P(x)=N\exp[-U(x)/\nu_{\rm th}^2]. \tag{34}$$

Using the analogy between our EFPE and Eq. (27), and following exactly the above-mentioned steps of Risken, we can derive the SPDF for our EFPE. For our EFPE, $P(x)$, D, and $\hat{D}$ become

$$P(x)=\exp\left[-\varepsilon\{U(x)+D_1(x)\}\Big/\frac{D_2(x)}{\gamma}\right]C_0(x), \tag{35}$$

$$D=\left(\frac{D_2(x)}{\gamma}\right)^{1/2}\frac{\partial}{\partial x}-\varepsilon\frac{d\{U(x)+D_1(x)\}}{dx}\Big/\left(\frac{D_2(x)}{\gamma}\right)^{1/2}, \tag{36}$$

$$\hat{D}=\left(\frac{D_2(x)}{\gamma}\right)^{1/2}\frac{\partial}{\partial x}+(1-\varepsilon)\times\frac{d\{U(x)+D_1(x)\}}{dx}\Big/\left(\frac{D_2(x)}{\gamma}\right)^{1/2}, \tag{37}$$

which are obtained by substituting the corresponding analogous terms in Eqs. (28), (30), and (31). For our EFPE, Eq. (32) becomes

$$\left[\left(\frac{D_2(x)}{\gamma}\right)^{1/2}\frac{\partial}{\partial x}+(1-\varepsilon)\times\frac{d\{U(x)+D_1(x)\}}{dx}\Big/\left(\frac{D_2(x)}{\gamma}\right)^{1/2}\right]C_0=0. \tag{38}$$

Solving for C_0, we have

$$\ln C_0=-\gamma(1-\varepsilon)\int\frac{\frac{d}{dx}\{U(x)+D_1(x)\}}{D_2(x)}dx. \tag{39}$$

Evaluation of the integral in Eq. (39) is computationally forbidding. However, it is observed that if $D_2(x)$ happens to be a slowly varying function of x, we can take $D_2(x)$ out of the integral and evaluate the rest of the integral. That effectively means that under the condition $\partial D_2(x)/\partial x\approx 0$, we obtain, from Eq. (39),

$$C_0(x)\sim\exp\left[-(1-\varepsilon)\{U(x)+D_1(x)\}\Big/\frac{D_2(x)}{\gamma}\right]. \tag{40}$$

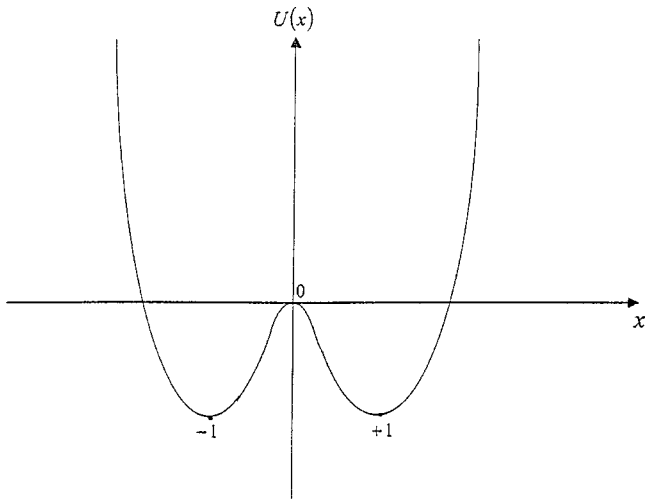

FIG. 1. The bistable potential.

With this approximation our stationary probability density function can be obtained by substituting Eq. (40) into Eq. (35) as

$$P(x)=N\exp\left[-\{U(x)+D_1(x)\}\Big/\frac{D_2(x)}{\gamma}\right], \tag{41}$$

where

$$N=\left\{\int_{-\infty}^{\infty}\exp\left[-\{U(x)+D_1(x)\}\Big/\frac{D_2(x)}{\gamma}\right]dx\right\}^{-1} \tag{42}$$

is the normalization constant.

With regard to our approximation $[\partial D_2(x)/\partial x\approx 0]$, we found in our numerical computation of $D_1(x)$ and $D_2(x)$ over the region $-2\leqslant x\leqslant 2$ (please see Sec. IV) that $D_2(x)$ indeed varies slowly with x as compared to $D_1(x)$, thus supporting our above approximation. Therefore, we propose Eq. (41) as the approximate SPDF for the solution process of one-dimensional damped stochastic system driven by OU noise under the condition that $[\partial D_2(x)/\partial x\approx 0]$.

IV. CASE STUDY: BISTABLE POTENTIAL

In order to validate our above theory, we take up the case study of damped bistable system driven by OU noise. The bistable potential shown in Fig. 1 is given by

$$U(x)=-\frac{x^2}{2}+\frac{x^4}{4}. \tag{43}$$

$x=-1$ and $x=+1$ are the two minima of the bistable potential.

For the case of bistable potential, our approximate FPE becomes Eq. (23), with

$$U'(x)=-x+x^3. \tag{44}$$

A. Numerical computation of MAP

In order to compute the effective diffusion coefficients $D_1(x)$ and $D_2(x)$ given by Eqs. (22), we have to first evalu-

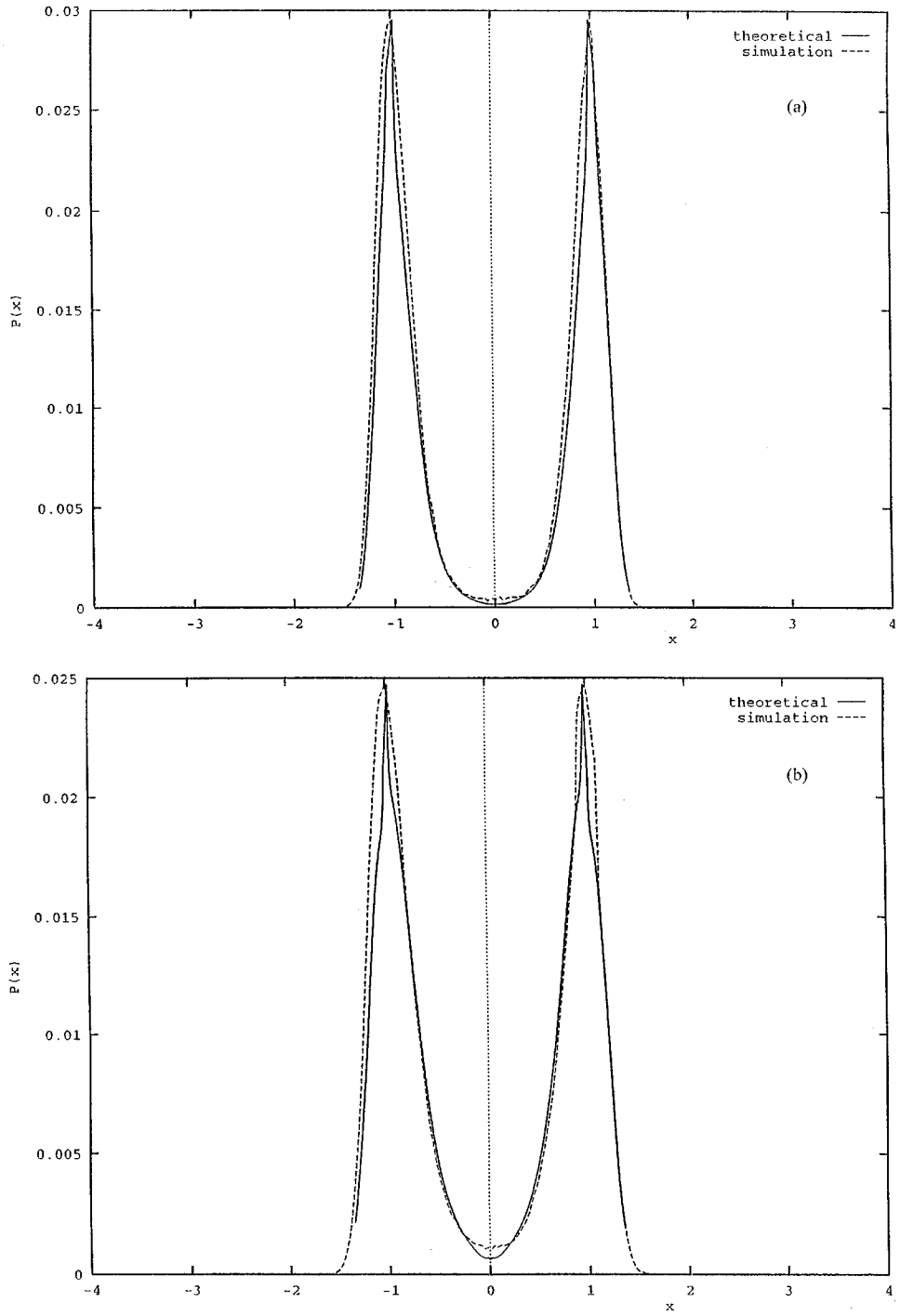

FIG. 2. (a) The SPDF of our theoretical results computed using Eq. (41) (solid lines) is compared with our digital simulation results (dashed lines) for $D=0.2$, $\gamma=3.5$, and $\tau=0.2$. (b) The SPDF of our theoretical results computed using Eq. (41) (solid lines) is compared with our digital simulation results (dashed lines) for $D=0.3$, $\gamma=3.5$, and $\tau=0.2$. (c) The SPDF of our theoretical results computed using Eq. (41) (solid lines) is compared with our digital simulation results (dashed lines) for $D=0.45$, $\gamma=3.5$, and $\tau=0.2$.

ate the velocity $y(x)$ along the MAP. In order to obtain the MAP, we need to solve the fourth order, nonlinear, ordinary differential equation given by Eq. (20) numerically with suitable boundary conditions. The MAP is that path which minimizes the action $S[x(t)]$ involved in reaching the point $x(t)=x$ from $x(0)$. It is valid to assume the Brownian particle to be at rest at the stable point (to whose basin of attraction x belongs) for a long time, before an optimal fluctuation takes it to x[38]. Since $x(0)$ is a stable point, the MAP becomes time-translational invariant. Therefore we let $t\rightarrow\infty$. For the case of bistable potential we then have $x(t\rightarrow\infty)=x$, $x(t=0)=+1$ for $0\leqslant x<\infty$, and $x(t=0)=-1$ for $-\infty<x<0$.

Numerical solution of Eq. (20) requires specifying four boundary conditions. Two of these boundary conditions are $y(x=-1)=0$ and $y(x=0)=0$, and they follow from the condition that the Brownian particle starts and finishes at rest. The remaining two boundary conditions are specified as the values of the derivatives at the end points, i.e., $y'(x=-1)$ and $y'(x=0)$ [34]. We obtain these boundary condi-

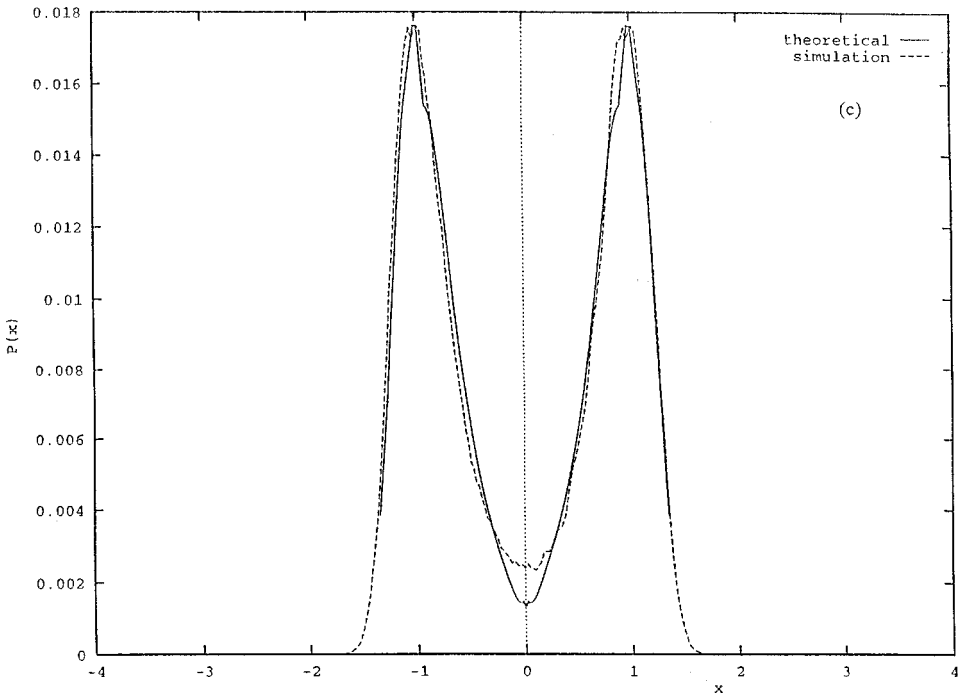

FIG. 2. (*Continued*).

tions by linearizing the sixth order nonlinear ordinary differential equation in $x(t)$, given by Eq. (19). The linearization is done around the minimum and the maximum points of the bistable potential. This lengthy procedure of evaluating the boundary conditions is deferred to the Appendix A. At the end of the procedure described in the Appendix A, we obtain the boundary conditions $y(x=-1)=0$, $y(x=0)=0$, $y'(x=-1)=\lambda_1$, and $y'(x=0)=\lambda_2$, where λ_1 is that eigenvalue which is real, positive and has the smallest magnitude, and λ_2 is that eigenvalue which is real, negative and has the smallest magnitude.

The fourth order nonlinear ordinary differential equation given by Eq. (20) with four boundary conditions specified at the starting and the ending points is known as a two point boundary value problem. We solve the two point boundary value problem given by Eq. (20) using the relaxation method [39]. Good initial guesses are the secret of efficient relaxation methods. No initial guess for the MAP of an underdamped colored noise driven bistable system is available (to our knowledge). Therefore we make use of the MAP for an overdamped colored noise driven bistable system in the small τ limit given by Eq. (15) in Ref. [30] for our initial guess. Keeping terms up to the order of τ^2 in Eq. (15) of Ref. [30], we have, $y=U'+2\tau^2U'^2U'''$. We use this y as the initial guess in our numerical procedure for the calculation of the MAP [Eq. (20)].

For finding the MAP in the region of x from $x=-1$ to -2, we treat the fourth order, nonlinear, ordinary differential equation given by Eq. (20) as an initial value problem. We solve Eq. (20) by applying fourth order Runge-Kutta method [39]. We cannot initialize our numerical computation procedure at $x=-1$, since the values of y and all its higher derivatives are zero at this point. This makes the initial value of the function given by Eq. (20) mathematically indeterminate at $x=-1$. So we take the starting point at $x=-1.01$, which is very close to the minimum $x=-1$. For the initial value of y at $x=-1.01$, we take $y(x=-1.01)=-y(x=-0.99)$. This is due to the symmetry of the solution near the minimum of the bistable potential, as the bistable potential is almost parabolic at the minimum point. The magnitudes of y', y'', and y''' at $x=-1.01$ are also assumed to be the same as their corresponding magnitudes at $x=-0.99$. The sign of y at $x=-1.01$ is taken to be negative as $y\leqslant 0$ for $-\infty<x\leqslant -1$. The signs of y', y'', and y''' at $x=-1.01$ are held positive, which is the simplest assumption made to keep the sign of y negative throughout the region $-2\leqslant x\leqslant -1$. As such the MAP calculation is mathematically nonuniform at the points $x=-1$ and $+1$. As a result the peaks of the probability distribution in our figures show notches and bumps. We thus solve Eq. (20) numerically, and find the MAP in the region $-2\leqslant x\leqslant 0$, enabling us to calculate the diffusion coefficients $D_1(x)$ and $D_2(x)$ over this whole region.

B. SPDF

The diffusion coefficients $D_1(x)$ and $D_2(x)$ calculated in Sec. IV A are used to compute the SPDF given by Eq. (41). We compute the SPDF $P(x)$ for $x<0$ for various values of D, γ, and τ using Eq. (41). SPDF's in the range $x>0$ are obtained immediately from the symmetry $P(-x)=P(x)$, thus obtaining $P(x)$ for $-2\leqslant x\leqslant 2$. For comparing our theoretical results, we also perform a digital simulation for the same sets of D, γ, and τ using the second order algorithm developed by Fox [40], and adapted by us (For details, please see Ref. [32]) for an OU noise driven damped bistable system. In order to obtain the normalized SPDF given by Eq. (41), we have to calculate the normalization constant N given by Eq. (42). Since $D_1(x)$ and $D_2(x)$ have been computed through our numerical procedure only over the limited range $-2\leqslant x\leqslant 2$, we are unable to compute N. In order to account for the unknown normalization constant, the peak of the un-

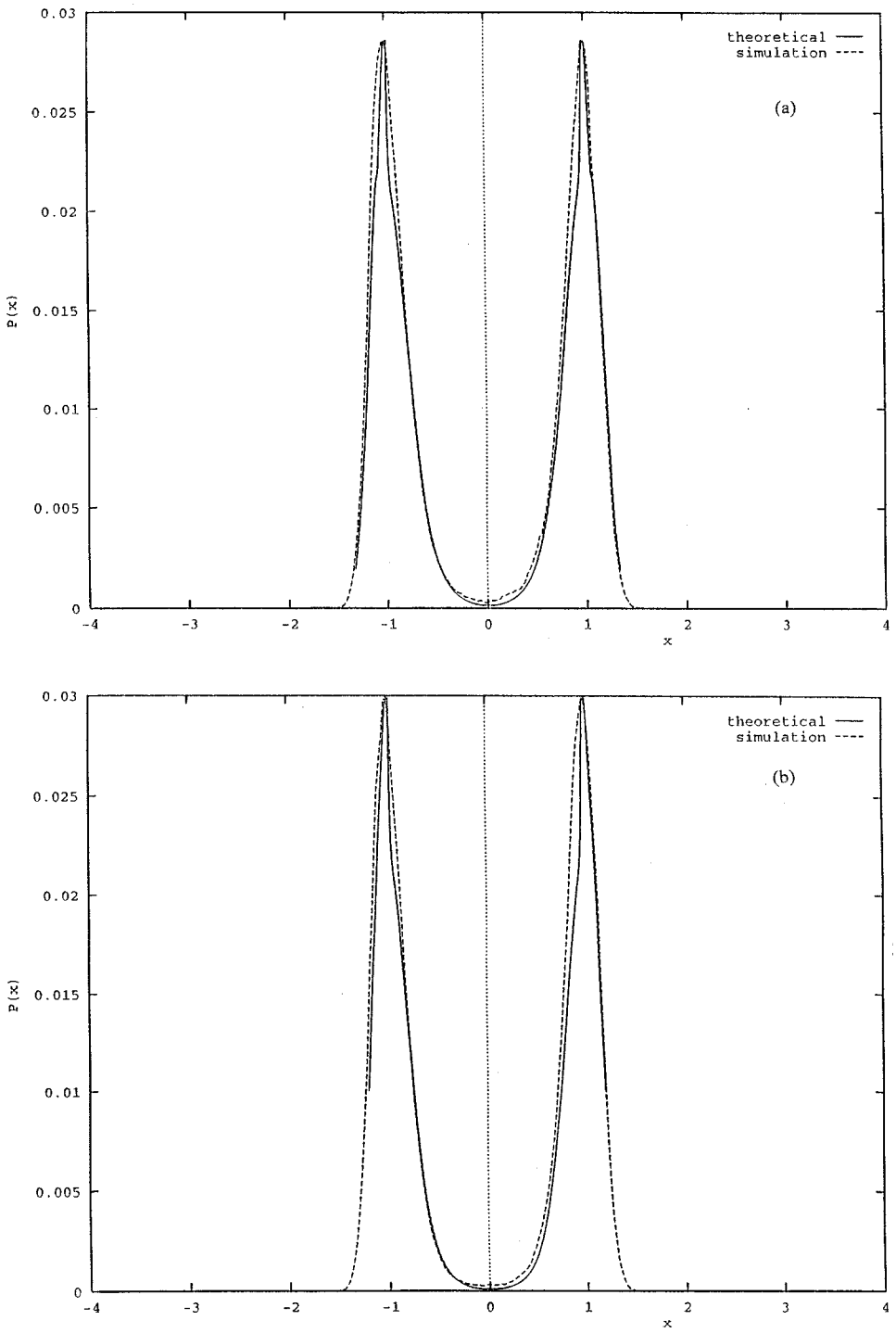

FIG. 3. (a) The SPDF of our theoretical results computed using Eq. (41) (solid lines) is compared with our digital simulation results (dashed lines) for $D=0.3$, $\gamma=5.0$, and $\tau=0.2$. (b) The SPDF of our theoretical results computed using Eq. (41) (solid lines) is compared with our digital simulation results (dashed lines) for $D=0.3$, $\gamma=5.5$, and $\tau=0.2$.

normalized theoretical SPDF is made to coincide with the peak of the normalized SPDF obtained through digital simulation.

In Figs. 2–4, the value of the SPDF $P(x)$, calculated using our approximate FPE as well as through digital simulation, is plotted against x for various values of D, γ, and τ. In Figs. 2(a)–2(c), the value of our SPDF $P(x)$ is plotted against x for various values of D with fixed γ and τ. In Figs. 3(a) and 3(b), we plot $P(x)$ against x for various values of γ by fixing D and τ. In Figs. 4(a) and 4(b), we plot $P(x)$ against x for different values of τ, keeping D and γ fixed.

Figures 2–4 show that our SPDF curves coincide favorably well with the digital simulation results (but for the normalizing constant). It is seen from Figs. 2(a)–2(c) that the SPDF curve becomes less peaked with increasing D at fixed γ and τ. This behavior of the SPDF curve is in qualitative agreement with the conclusions drawn from digital simulation. In Figs. 2(b), 3(a), and 3(b), it is observed that with increasing γ at fixed D and τ, the SPDF curve becomes more peaked, establishing complete agreement with the inference drawn from the digital simulation results. In Figs. 2(a), 4(a), and 4(b), we note that the peak of the SPDF curve increases with increasing τ at fixed D and γ, showing exactly the same behavior as in the case of digital simulation results. It is thus seen that the SPDF obtained through our approximate FPE is in good agreement with the corresponding digital simulation

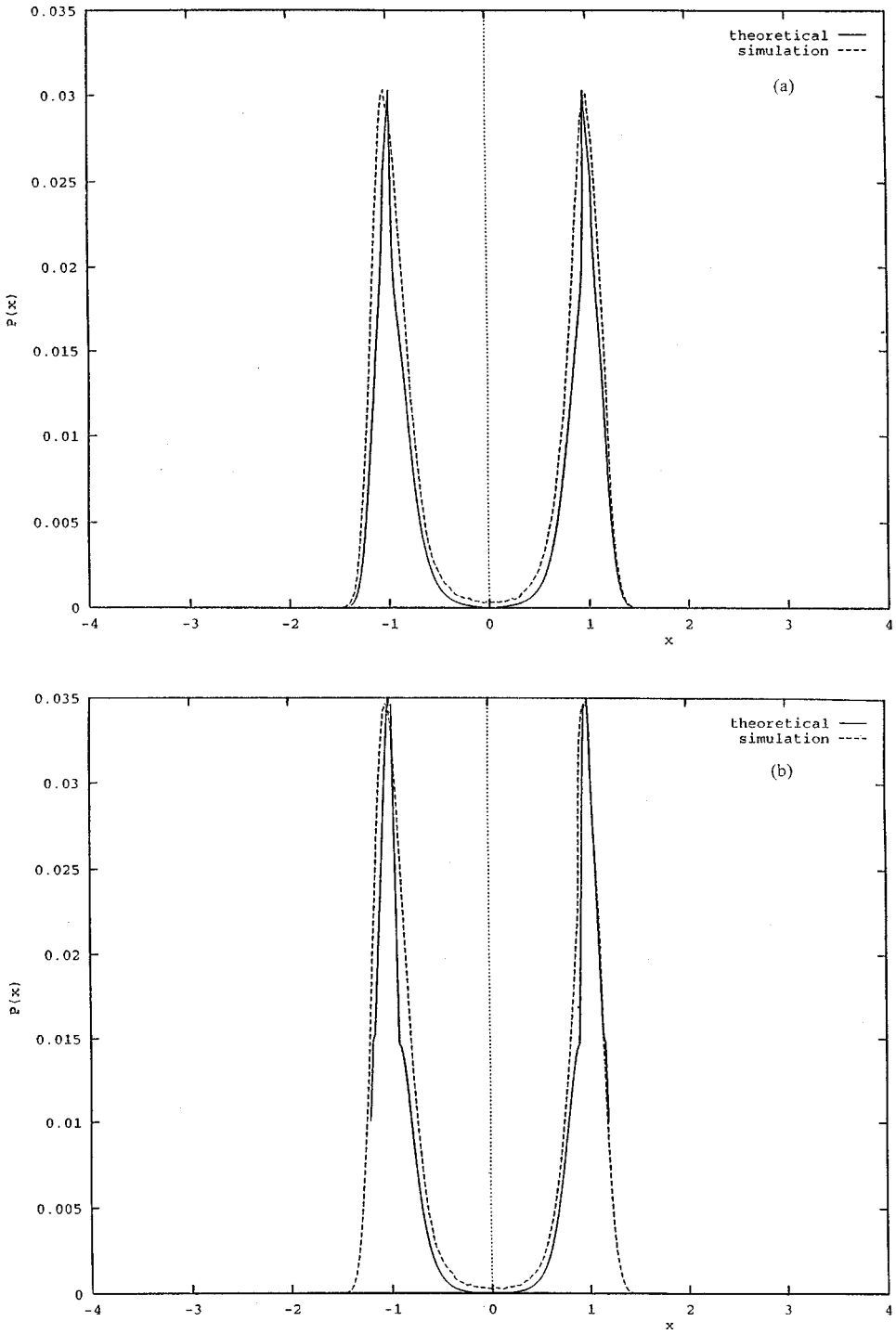

FIG. 4. (a) The SPDF of our theoretical results computed using Eq. (41) (solid lines) is compared with our digital simulation results (dashed lines) for $D=0.2$, $\gamma=3.5$, and $\tau=0.4$. (b) The SPDF of our theoretical results computed using Eq. (41) (solid lines) is compared with our digital simulation results (dashed lines) for $D=0.2$, $\gamma=3.5$, and $\tau=0.5$.

result.

With regard to the effectiveness of our theoretical prediction with a change in the parameters, we can draw the following conclusions. From Figs. 2(a)–2(c), it can be seen that as $D\rightarrow 0$ our theory follows our digital simulation more closely. This can be inferred from the fact that the theoretical SPDF coincides better with the digitally simulated SPDF at $x=0$ for smaller D, keeping in mind that the two SPDFs are made to coincide at the peaks for the sake of normalization. From Figs. 2(b), 3(a), and 3(b), we note that our theoretical predictions are not affected appreciably with a change in γ. From Figs. 2(a), 4(a), and 4(b), and from a comparison of SPDF obtained through digital simulation with our theory done for larger τ (which are not reported here), we note that our theoretical predictions are better only when τ is small.

V. CONCLUSIONS

This paper has concentrated on developing an analytical solution to the problem of damped stochastic system driven by colored noise. We briefly summarize the procedure adopted by us. We derive our EFPE starting with an exact master equation for the probability density in position and velocity space obtained by using the functional derivative technique. In the limit $D\rightarrow 0$, the major contribution to the path integrals occurring in the EFPE arises around the MAP,

which minimizes the action of the Brownian particle in reaching the maximum of the potential. Using the MAP, the effective diffusion coefficients $D_1(x)$ and $D_2(x)$ associated with the EFPE are derived. We find that our EFPE is analogous to the FPE describing a damped stochastic system driven by Gaussian white noise. This analogy is used along with the MCF method [2] in obtaining the formula for the SPDF.

Our proposed theory is validated by taking up the case study of damped bistable system driven by OU noise. The MAP is computed by solving a fourth order, nonlinear, ordinary differential equation using a numerical method imposing suitable boundary conditions. The boundary conditions are obtained by linearizing a sixth order, nonlinear, ordinary differential equation. Effective diffusion coefficients $D_1(x)$ and $D_2(x)$ are calculated in the range $-2 \leqslant x \leqslant 2$ using the MAP. The SPDF is then computed using our theoretical formula for various values of D, γ, and τ.

For the purpose of comparing our theoretical results, we perform a digital simulation of the damped bistable system driven by OU noise using Fox's second order algorithm. It is observed that our theoretical results for the SPDF agree favorably with our corresponding digital simulation results.

Although our formula for the effective diffusion coefficients associated with the EFPE is valid for general values of parameters D, γ, and τ, we could validate the formula only over a limited range of parameters for the following reasons: (a) In our numerical computation of the MAP, we have to choose only such values of γ for which the rate constant λ becomes real and nonoscillatory [refer to Eq. (A12)]. This limits the range of γ for which our numerical procedure can be applied. (b) Further, our numerical method for the calculation of the MAP shows a diverging behavior for very small as well as very large values of τ. (c) Moreover, our theory of the EFPE is valid only in the limit $D \to 0$. Because of these three restrictions, we could vary our parameters D, γ, and τ effectively only within a limited range. Therefore, we could not compare our theory with digital simulations over a wider range of parameters. However within its limited range our theory compares favorably with our digital simulation results.

ACKNOWLEDGMENTS

We thank Professor M. Gopal, Department of Electrical Engineering, Indian Institute of Technology, Delhi for his continuous help and encouragement. C.M. thanks Indian Institute of Technology, Madras for the hospitality provided to her during the latter part of this research work.

APPENDIX

In this Appendix we obtain the boundary conditions $y'(x=-1)$ and $y'(x=0)$ necessary for solving the MAP given by Eq. (20). The derivatives $y'(x=-1)$ and $y'(x=0)$ are evaluated from the sixth order, nonlinear ordinary differential equation in $x(t)$ given by the extremal condition $\delta S[x(t)]/\delta x(t)=0$ [Eq. (19)] for the action $S[x(t)]$ given by Eq. (18). Equations (18) and (19) yield the following sixth order, nonlinear ordinary differential equation in $x(t)$:

$$x^{vi}=\frac{2}{\tau^2}U''\ddot{x}+\frac{1}{\tau^2}U'U''-\frac{\gamma^2}{\tau^2}\ddot{x}-2U''x^{iv}-U''U'''\dot{x}^2-U''^2\ddot{x}$$
$$+\frac{1}{\tau^2}x^{iv}+\frac{1}{\tau^2}U'''\dot{x}^2+\gamma^2x^{iv}+\gamma U''''\dot{x}^3+3\gamma U'''\dot{x}\ddot{x}$$
$$-U''''\dot{x}^4-6U''''\dot{x}^2\ddot{x}-3U'''\ddot{x}^2-4U'''\dot{x}\dddot{x} \tag{A1}$$

where $\dot{x}$, $\ddot{x}$, $\dddot{x}$, x^{iv}, x^v, and x^{vi} denote first, second, third, fourth, fifth, and sixth order derivatives of x with respect to time.

By letting

$$x_1=x, \quad x_2=\dot{x}, \quad x_3=\ddot{x}, \quad x_4=\dddot{x}, \quad x_5=x^{iv}, \quad x_6=x^v, \tag{A2}$$

Eq. (A1) can be reduced to a set of six first-order differential equations given below:

$$\dot{x}_1=x_2=f_1(x_1,x_2,x_3,x_4,x_5,x_6),$$
$$\dot{x}_2=x_3=f_2(x_1,x_2,x_3,x_4,x_5,x_6),$$
$$\dot{x}_3=x_4=f_3(x_1,x_2,x_3,x_4,x_5,x_6),$$
$$\dot{x}_4=x_5=f_4(x_1,x_2,x_3,x_4,x_5,x_6),$$
$$\dot{x}_5=x_6=f_5(x_1,x_2,x_3,x_4,x_5,x_6),$$

$$\dot{x}_6=\frac{2}{\tau^2}U''\ddot{x}+\frac{1}{\tau^2}U'U''-\frac{\gamma^2}{\tau^2}\ddot{x}-2U''x^{iv}-U''U'''\dot{x}^2-U''^2\ddot{x}$$
$$+\frac{1}{\tau^2}x^{iv}+\frac{1}{\tau^2}U'''\dot{x}^2+\gamma^2x^{iv}+\gamma U''''\dot{x}^3+3\gamma U'''\dot{x}\ddot{x}$$
$$-U''''\dot{x}^4-6U''''\dot{x}^2\ddot{x}-3U'''\ddot{x}^2-4U'''\dot{x}\dddot{x}$$
$$=f_6(x_1,x_2,x_3,x_4,x_5,x_6), \tag{A3}$$

The above equations can be written as the state equation

$$\dot{\mathbf{X}}=\mathbf{f}(\mathbf{X}), \tag{A4}$$

where

$$\mathbf{X}=[x_1 \quad x_2 \quad x_3 \quad x_4 \quad x_5 \quad x_6]^T \tag{A5}$$

and

$$f(\mathbf{X})=[f_1(\mathbf{X}) \quad f_2(\mathbf{X}) \quad f_3(\mathbf{X}) \quad f_4(\mathbf{X}) \quad f_5(\mathbf{X}) \quad f_6(\mathbf{X})]^T. \tag{A6}$$

Equation (A4) can be linearized for small variations about an equilibrium point $\mathbf{X}_0$. The derivatives of all the state variables are zero at the equilibrium point $\mathbf{X}_0$. Expanding Eq. (A4) into a Taylor series, and neglecting terms of second and higher orders, for the ith state equation we obtain

$$x_i=f_i(\mathbf{X}_0)+\sum_{j=1}^{n}\left.\frac{\partial f_i(\mathbf{X})}{\partial x_j}\right|_{\mathbf{x}=\mathbf{x}_0}(x_j-x_{j0}). \tag{A7}$$

Recognizing that at the equilibrium point, $\mathbf{f}_i(\mathbf{X}_0)=0$, and defining the variation about the equilibrium point as $\tilde{x}_j=x_j-x_{j0}$, we obtain $\dot{\tilde{x}}_j=\dot{x}_j$.

The linearized state equation can be written as

$$\dot{\tilde{x}}_i = \sum_{j=1}^{n} \left. \frac{\partial f_i(\mathbf{X})}{\partial x_j} \right|_{\mathbf{x}=\mathbf{x}_0} \tilde{x}_j . \tag{A8}$$

The above linearized component equation given in Eq. (A8) can be written as the vector matrix equation

$$\dot{\tilde{\mathbf{X}}} = A\tilde{\mathbf{X}}, \tag{A9}$$

where

$$\mathbf{A} = \begin{bmatrix} \frac{\partial f_1}{\partial x_1} & \frac{\partial f_1}{\partial x_2} & \cdots & \frac{\partial f_1}{\partial x_n} \\ \frac{\partial f_2}{\partial x_1} & \frac{\partial f_2}{\partial x_2} & \cdots & \frac{\partial f_2}{\partial x_n} \\ \cdots\cdots\cdots\cdots\cdots\cdots\cdots\cdots \\ \frac{\partial f_n}{\partial x_1} & \frac{\partial f_n}{\partial x_2} & \cdots & \frac{\partial f_n}{\partial x_n} \end{bmatrix} .$$

All the partial derivatives in matrix $\mathbf{A}$ are evaluated at the equilibrium state $\mathbf{X}_0$.

Applying the above linearizing procedure to our nonlinear equation given by Eq. (A1), with the equilibrium point taken at the minimum of the bistable potential $x=-1$, we obtain the state equation

$$\dot{\tilde{\mathbf{X}}} = \mathbf{A}\tilde{\mathbf{X}}, \tag{A10}$$

where

$$\mathbf{A} = \begin{bmatrix} 0 & 1 & 0 & 0 & 0 & 0 \\ 0 & 0 & 1 & 0 & 0 & 0 \\ 0 & 0 & 0 & 1 & 0 & 0 \\ 0 & 0 & 0 & 0 & 1 & 0 \\ 0 & 0 & 0 & 0 & 0 & 1 \\ \frac{\partial f_6}{\partial x_1} & \frac{\partial f_6}{\partial x_2} & \frac{\partial f_6}{\partial x_3} & \frac{\partial f_6}{\partial x_4} & \frac{\partial f_6}{\partial x_5} & \frac{\partial f_6}{\partial x_6} \end{bmatrix}$$

Matrix $\mathbf{A}$ has six distinct eigen values $\lambda_1 \ldots, \lambda_6$. Now, the solution of Eq. (A10) is given by

$$\tilde{\mathbf{X}}(t) = e^{\mathbf{A}t}\tilde{\mathbf{X}}_0 = \mathbf{M}e^{\mathbf{L}t}\mathbf{M}^{-1}\tilde{\mathbf{X}}_0 , \tag{A11}$$

where $\mathbf{M}$ is the diagonalizing or modal matrix [41], and $\mathbf{L}$ is a diagonal matrix given by

$$\mathbf{L} = \begin{bmatrix} \lambda_1 & 0 & 0 & 0 & 0 & 0 \\ 0 & \lambda_2 & 0 & 0 & 0 & 0 \\ 0 & 0 & \lambda_3 & 0 & 0 & 0 \\ 0 & 0 & 0 & \lambda_4 & 0 & 0 \\ 0 & 0 & 0 & 0 & \lambda_5 & 0 \\ 0 & 0 & 0 & 0 & 0 & \lambda_6 \end{bmatrix}$$

$\tilde{\mathbf{X}}_0$ is the initial state at $x=-1$. From Eq. (A11), we can finally obtain a general solution for x of the form

$$x-(-1) = \sum_{i=1}^{6} \alpha_i \exp(\lambda_i t)(i=1,...,6),$$

[34], with rate constants

$$\lambda_i = \pm\frac{1}{\tau}, \quad \pm\left(\frac{(\gamma^2-4)+\gamma\sqrt{\gamma^2-8}}{2}\right)^{1/2}, \quad \pm\left(\frac{(\gamma^2-4)-\gamma\sqrt{\gamma^2-8}}{2}\right)^{1/2} \tag{A12}$$

The condition for the solution to vanish for $t\to-\infty$ and be nonoscillatory demands that the solution has only those terms for which λ_i is positive and real. Furthermore, terms with λ_i having the smallest positive real part, say λ_1, will dominate the solution asymptotically. Then $x-(-1) \sim \exp(\lambda_1 t)$ which implies $y \equiv \dot{x} \to y = \lambda_1[x-(-1)]$. This gives the boundary condition $y'(x=-1)=\lambda_1$.

Similarly, linearizing Eq. (19) for x near 0 gives rise to a solution of the form $0-x=\sum_{i=1}^{6}\alpha_i \exp(\lambda_i t)$ $(i=1,...,6)$, with rate constants

$$\lambda_i = \pm\frac{1}{\tau}, \quad \pm\left(\frac{(\gamma^2+2)+\gamma\sqrt{\gamma^2+4}}{2}\right)^{1/2}, \quad \pm\left(\frac{(\gamma^2+2)-\gamma\sqrt{\gamma^2+4}}{2}\right)^{1/2}. \tag{A13}$$

Following similar reasoning as explained above, for a well-behaved solution we find that $y'(x=0)=\lambda_2$, where λ_2 is that eigenvalue which is real, negative, and has the smallest magnitude. Thus the boundary conditions $y(x=-1)=0$, $y(x=0)=0$, $y'(x=-1)$, and $y'(x=0)$ are obtained as mentioned above.

[1] N. G. Van Kampen, *Stochastic Processes in Physics and Chemistry* (North-Holland, Amsterdam, 1981).

[2] H. Risken, *The Fokker-Planck Equation—Methods of Solution and Applications* (Springer-Verlag, Berlin, 1984).

[3] *Noise in Nonlinear Dynamical System*, edited by F. Moss and P. V. E. McClintock (Cambridge University Press, Cambridge, 1989), Vols. I, II, and III; P. Hanggi, P. Jung, and F. Marchesoni, J. Stat. Phys. **54**, 1367 (1989); H. Risken, G. Debnath, F. Moss, Th. Leiber, and F. Marchesoni, Phys. Rev. A **42**, 703 (1990); P. Jung and P. Hanggi, Adv. Chem. Phys. **89**, 239 (1995); F. Marchesoni, Phys. Rev. Lett. **77**, 787 (1996).

[4] W. Dieterich, P. Fulde, and I. Peschel, Adv. Phys. **29**, 527 (1980).

[5] R. Ferrando, R. Spadacini, and G. E. Tommei, Phys. Rev. B **45**, 444 (1992).

[6] E. G. Gwinn and R. M. Westervelt, Phys. Rev. Lett. **54**, 1613 (1985), and references therein; S. W. Teitsworth and R. M. Westervelt, *ibid.* **56**, 516 (1986).

[7] S. Kai, in *Noise in Nonlinear Dynamical Systems* (Ref. [3]) Vol. III.
[8] M. Schumaker and W. Horsthemke, J. Stat. Phys. **54**, 1189 (1989).
[9] R. Graham, M. Hohnerbach, and A. Schenzle, Phys. Rev. Lett. **48**, 1396 (1982); F. T. Arecchi, R. Meucci, G. Puccioni, and J. Tredicce, *ibid.* **49**, 1217 (1982); N. B. Abraham, L. A. Lugiato, and L. M. Narducci, Phys. Today **39(1)**, S53 (1986).
[10] W. W. Chow, J. Gea-Banacloche, L. M. Pedrotti, V. E. Sanders, W. Schleich, and M. O. Scully, Rev. Mod. Phys. **57**, 61 (1985), and references therein.
[11] Y. M. Golubev and M. I. Kolobov, Phys. Rev. Lett. **79**, 399 (1997).
[12] P. Hanggi, P. Talkner, and M. Borkovec, Rev. Mod. Phys. **62**, 251 (1990).
[13] A. Nitzan and J. Ross, J. Chem. Phys. **59**, 241 (1973).
[14] S. Kabashima, S. Kogure, T. Kawakubo, and T. Okada, J. Appl. Phys. **50**, 6296 (1979).
[15] *Noise and Nonlinear Phenomena in Nuclear Systems*, edited by J. L. Munoz-Cobo and F. C. Difilippo (Plenum, New York, 1989).
[16] R. P. Garay and R. Lefever, J. Theor. Biol. **73**, 417 (1978).
[17] M. Kimura and T. Ohta, *Theoretical Aspects of Population Genetics* (Princeton University Press, Princeton, 1991).
[18] W. C. Schieve, A. R. Bulsara, and G. M. Davis, Phys. Rev. A **43**, 2613 (1991).
[19] W. Alt, J. Math. Biol. **9**, 147 (1980); BioSystems **34**, 11 (1985); M. Schienbein and H. Gruler, Bull. Math. Biol. **55**, 585 (1993); R. Dickinson and R. T. Tranquillo, J. Math. Biol. **31**, 563 (1993).
[20] H. Frauenfelder and P. G. Wolynes, Science **229**, 337 (1985); D. L. Stein, Proc. Natl. Acad. Sci. USA **82**, 3670 (1985).
[21] W. Horsthemke and R. Lefever, *Noise-Induced Transitions, Theory and Applications in Physics, Chemistry, and Biology* (Springer-Verlag, Berlin, 1984).
[22] E. A. Novikov, Zh. Eksp. Teor. Fiz. **47**, 30 (1964) [Sov. Phys. JETP **20**, 1290 (1965)]; J. M. Sancho, M. San Miguel, S. L. Katz, and J. D. Gunton, Phys. Rev. A **26**, 1589 (1982); R. F. Fox, *ibid.* **33**, 467 (1986); **34**, 4525 (1986).
[23] N. G. Van Kampen, Physica (Utrecht) **74**, 215 (1974).
[24] P. Grigolini, Phys. Lett. A **119**, 157 (1986); P. Grigolini and F. Marchesoni, Physica A **121**, 269 (1983).
[25] P. Jung and P. Hanggi, Phys. Rev. Lett. **61**, 11 (1988).
[26] A. J. Bray and A. J. McKane, Phys. Rev. Lett. **62**, 493 (1989); A. J. McKane, H. C. Luckock, and A. J. Bray, Phys. Rev. A **41**, 644 (1990); A. J. Bray, A. J. McKane, and T. J. Newman, *ibid.* **41**, 657 (1990); H. C. Luckock and A. J. McKane, *ibid.* **42**, 1982 (1990); K. M. Rattray and A. J. McKane, J. Phys. A **24**, 4375 (1991).
[27] L. Pesquera, M. A. Rodriguez, and E. Santos, Phys. Lett. **94A**, 287 (1983); Horacio S. Wio, P. Colet, M. San Miguel, L. Pesquera, and M. A. Rodriguez, Phys. Rev. A **40**, 7312 (1989).
[28] P. Hanggi, Z. Phys. B: Condens. Matter **75**, 275 (1989); M. I. Dykman, Phys. Rev. A **42**, 2020 (1990).
[29] J. F. Luciani and A. D. Verga, J. Stat. Phys. **50**, 567 (1988).
[30] T. G. Venkatesh and L. M. Patnaik, Phys. Rev. E **48**, 2402 (1993); Phys. Rev. A **46**, R7355 (1992); Phys. Rev. E **47**, 1589 (1993).
[31] F. Marchesoni, E. Menichella-Saetta, M. Pochini, and S. Santucci, Phys. Rev. A **37**, 3058 (1988); Phys. Lett. A **130**, 467 (1988); F. Marchesoni, *ibid.* **237**, 126 (1998); L. Gammaitoni, E. Menichella-Saetta, F. Marchesoni, and G. Presilla, Phys. Rev. A **40**, 2105 (1989); Rev. Mod. Phys. **70**, 223 (1998).
[32] Chitralekha Mahanta and T. G. Venkatesh, Phys. Rev. E **58**, 4141 (1998).
[33] L. Fronzoni, P. Grigolini, P. Hanggi, F. Moss, R. Mannella, and P. V. E. McClintock, Phys. Rev. A **33**, 3320 (1986).
[34] T. J. Newman, A. J. Bray, and A. J. McKane, J. Stat. Phys. **59**, 357 (1990).
[35] P. Hanggi, Z. Phys. B: Condens. Matter **31**, 407 (1978).
[36] *Stochastic Processes Applied to Physics*, edited by L. Pesquera and M. Rodriguez (World Scientific, Singapore, 1985), pp. 69–95.
[37] L. Ramirez-Piscina and J. M. Sancho, Phys. Rev. A **37**, 4469 (1988).
[38] M. I. Dykman, Phys. Rev. A **42**, 2020 (1990); A. Foster and A. S. Mikhailov, Phys. Lett. A **126**, 459 (1988).
[39] W. H. Press, S. A. Teukolsky, W. T. Vetterling, and B. P. Flannery, *Numerical Recipes in C, the Art of Scientific Computing*, 2nd ed. (Cambridge University Press, Cambridge, 1997).
[40] R. F. Fox, Phys. Rev. A **43**, 2649 (1991).
[41] Francis B. Hildebrand, *Methods of Applied Mathematics*, 2nd ed. (Prentice-Hall of India, New Delhi, 1968).